



Cite this: *Nanoscale Adv.*, 2021, **3**, 1997

## Response of G protein-coupled receptor CED-1 in germline to polystyrene nanoparticles in *Caenorhabditis elegans*†

Yunhan Yang, Wenting Dong, Qiuli Wu \* and Dayong Wang \*

The deposition of a certain amount of nanopolystyrene (NPS) can be observed in the gonad of *Caenorhabditis elegans*. However, we still know little about the response of germline towards NPS exposure. In the germline of *C. elegans*, NPS (1–1000  $\mu\text{g L}^{-1}$ ) increased the expression levels of two G protein-coupled receptors (GPCRs), namely PAQR-2 and CED-1. Moreover, susceptibility to NPS toxicity was observed in *ced-1(RNAi)* worms, which suggested that the protective response of germline was mediated by GPCR CED-1. In the germline, five proteins (CED-10, VPS-34, SNX-1, RAB-7, and RAB-14) functioned as downstream targets of GPCR CED-1 in controlling NPS toxicity. Furthermore, these five targets in the germline regulated NPS toxicity by affecting the activities of p38 MAPK and insulin signaling pathways in intestinal cells. Therefore, we raised a GPCR CED-1-mediated signaling cascade in the germline in response to NPS exposure, which is helpful for understanding the molecular basis of the germline in response to NPS exposure.

Received 16th October 2020

Accepted 16th February 2021

DOI: 10.1039/d0na00867b

[rsc.li/nanoscale-advances](http://rsc.li/nanoscale-advances)

## 1. Introduction

Based on the observations of ubiquity and degradation into smaller particles (microplastics (MP) or nanoplastics (NP)), it has been gradually recognized that plastic pollution is already a serious environmental concern.<sup>1,2</sup> Moreover, a growing number of literature on exposure to MP or NP have indicated their adverse effects on biota.<sup>3,4</sup> Exposure to MP or NP could potentially induce damage to development, movement activity, immune system, reproductive capacity, etc.<sup>5–8</sup> A few determining factors, including particle size, exposure concentration, exposure duration, species, and polymer type, can affect the toxicity induction of MP or NP.<sup>9</sup> After the exposure, the determination of MP or NP toxicity was closely related to the activation of oxidative stress in organisms.<sup>10,11</sup>

The NP particles are supposed to be abundant in different environments (such as aquatic environments) due to their role at the expected lower end of size distribution.<sup>12</sup> The emergence of possible impacts due to NP exposure on environmental animals and humans has received increasing attention.<sup>13</sup> Recently, the nematode *Caenorhabditis elegans* has been applied for the evaluation of NP toxicity.<sup>14,15</sup> It is an animal model having sensitivity towards numerous environmental exposures.<sup>16</sup> Potential exposure to NP particles induces at least reproductive toxicity, intestinal toxicity, and neurotoxicity in *C. elegans*.<sup>17–19</sup> After exposure, the NP particles could not only be

accumulated in the intestinal lumen but could also further be translocated and enriched in the gonad of nematodes.<sup>20,21</sup>

Bioavailable environmental toxicants normally induce the response by inhibiting or activating some G protein-coupled receptors (GPCRs) on the cytoplasmic membrane.<sup>22,23</sup> *C. elegans* is a powerful model to examine the molecular response of GPCRs towards toxicants.<sup>24</sup> A certain number of GPCRs has been identified in different tissues to control stress response towards toxicants.<sup>25</sup> For example, the intestinal GPCR of DAF-2 regulated nanoplastic toxicity by activating the downstream signaling cascade of AGE-1-AKT-1-DAF-16.<sup>26</sup> Nevertheless, GPCRs in the germline dysregulated by the NP exposure are largely unclear in organisms.

The primary goal of this study is to determine GPCRs in the germline required for controlling response towards NP. Specific goals are: (i) to identify germline GPCRs dysregulated by NP exposure; (ii) to examine the role of germline GPCRs in controlling responses towards NP, and (iii) to determine the molecular basis for germline GPCRs in controlling NP toxicity. Nanopolystyrene (NPS) can be potentially used in at least food containers, packaging, textiles, and adhesives.<sup>27–29</sup> Thus, we selected NPS as the model NP and *C. elegans* as the animal model. We hypothesized that specific GPCRs existed in the germline required for response towards NPS. We also raised the evidence that GPCR CED-1 mediated the response of worms in the germline to the NPS exposure.

## 2. Experimental section

### NPS characterizations

NPS (100 nm) suspended in water was purchased from Janus New-Materials Co. (Nanjing, China). The transmission electron

Medical School, Southeast University, Nanjing 210009, China. E-mail: [qlwu@seu.edu.cn](mailto:qlwu@seu.edu.cn); [dayongw@seu.edu.cn](mailto:dayongw@seu.edu.cn)

† Electronic supplementary information (ESI) available. See DOI: [10.1039/d0na00867b](https://doi.org/10.1039/d0na00867b)



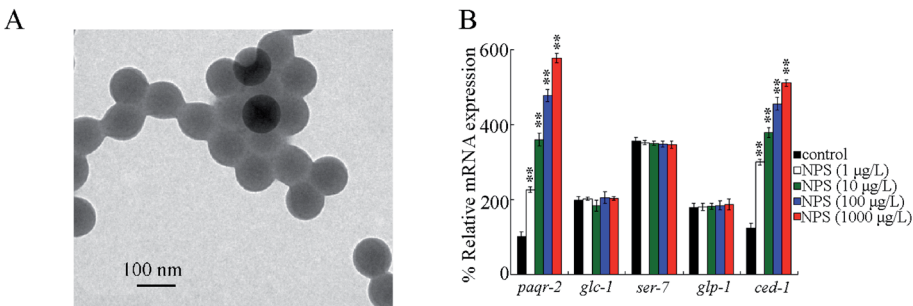


**Fig. 1** Identification of the germline GPCRs in response to NPS exposure in wild-type nematodes. (A) TEM image of NPS in the K medium before sonication. (B) Effect of NPS exposure on the expressions of genes encoding germline GPCRs in wild-type nematodes. Approximately 40 intact gonads were isolated for the extraction of total RNAs. Bars represent means  $\pm$  SD. \*\* $P$  < 0.01 vs. control. Statistical significance of differences between treatments was examined using one-way ANOVA.

microscopy (TEM) image of NPS before sonication is given in Fig. 1A, which shows the spherical morphology of NPS. Some other properties of this commercial NPS have been described in previous studies *via* Fourier transform infrared (FTIR) spectroscopy and Raman spectroscopy.<sup>30,31</sup> The zeta potential measurement indicated the value of  $-9.143 \pm 0.258$  mV for NPS. The dynamic light scattering (DLS) measurement indicated that the size of NPS was  $102.55 \pm 3.8$  nm. Working concentrations for NPS suspensions were  $1\text{--}1000 \mu\text{g L}^{-1}$ . Before the exposure, the working NPS suspensions were sonicated at 40 kHz (100 W) for 30 min. After sonication, the NPS suspensions did not show obvious aggregation for at least two days.<sup>26,30</sup>

### Strains and cultivation

The worm strains (unless otherwise described) and *Escherichia coli* strains (HT115 and OP50) were from the Caenorhabditis Genetics Center. Information for *C. elegans* strains is given in Table S1.† *C. elegans* was cultured as per standard procedure on nematode growth medium (NGM) agar seeded with OP50 in Petri dishes.<sup>32</sup> To obtain a synchronized L1-larvae population, gravid worms were treated with a bleaching solution containing NaOH (0.45 M) and 2% HOCl (2%) to release enough eggs on NGM plates.<sup>33</sup> Following that, the eggs were allowed to develop into L1 larvae.

### NPS exposure

The synchronized L1 larval worms were transferred and exposed in NPS suspensions added with OP50 ( $\sim 4 \times 10^6$  CFUs) to adult day-3 (approximately 6.5 days).<sup>30</sup> The liquid PS-NP suspensions were used for exposure. NPS suspensions were refreshed daily during the exposure process by transferring worms into new liquid PS-NP suspensions. During the NPS exposure, we did not observe clear developmental defects.

### Assessment endpoints

The production of reactive oxygen species (ROS) was applied in order to reflect the induction of oxidative stress.<sup>34</sup> *C. elegans* was treated for 3 h with CM-H<sub>2</sub>DCFDA (1 µM) in darkness, followed by washing using M9 buffer. Fluorescent signals in *C. elegans* were observed at 510 nm (emission filter)/488 nm (excitation

wavelength) under a laser scanning confocal microscope. In worms, the strongest ROS fluorescent signals are located in the intestine. Intestinal fluorescence intensities were analyzed by normalization against autofluorescence. For each exposure, 50 worms were determined.

The locomotion behavior was used to indicate the possible neurotoxicity of NPS.<sup>35</sup> *C. elegans* was first washed with the M9 buffer, and after further recovery on the NGM plate for 1 min, their locomotion behaviors were analyzed under a dissecting microscope. To determine the head thrash, alteration in the direction of posterior bulb along the *y*-axis was analyzed, assuming that the traveling direction was along the *x*-axis. To determine the body bend, alteration in the bending direction at mid-body was analyzed. For each exposure, 40 worms were determined.

Brood size can reflect the reproductive capacity in worms.<sup>16</sup> The brood size was counted as the number of offsprings at all stages beyond the egg under an optical microscope.<sup>31</sup> For each exposure, 30 worms were examined.

### Quantitative real-time polymerase chain reaction (qRT-PCR)

The worms were first ground in liquid nitrogen. Total RNA was extracted using TRIZOL (Invitrogen) according to the manufacturer's protocol. The concentration and purity of extracted RNAs were further determined using a spectrophotometer. The complementary DNA (cDNA) was synthesized from the same amount of total RNAs in the reverse transcriptase reaction using a Superscript III first-strain synthesis system (Invitrogen). qPCR was carried out with the StepOnePlus™ real-time PCR system using gene-specific primers (Table S2†) and SYBR Green qRT-PCR master mix in order to determine the transcriptional expressions of examined genes. The relative mRNA expressions were examined by normalization against the mRNA of TBA-1, an alpha-tubulin protein. Three independent experiments were then carried out.

### RNA interference (RNAi)

RNAi experiments were carried out by feeding *C. elegans* with bacteria (HT115) expressing double-stranded (ds) RNAs of *PAQR-2*, *CED-1*, *CED-10*, *VPS-34*, *SNX-1*, *RAB-7* or *RAB-14*.<sup>36</sup>



Before the growth on NGM plates, HT115 was transferred into an LA broth (LB broth containing 100  $\mu\text{g L}^{-1}$  ampicillin) with the addition of 5 mM isopropyl 1-thio- $\beta$ -D-galactopyranoside (IPTG). Then, the L1 larvae were cultured on RNAi plates with specific RNAi clones or an empty RNAi vector (L4440). The next generation was used for exposure to NPS. The DCL569 strain was a tool for the germline RNAi knockdown.<sup>37</sup> The RNAi knockdown efficiency was confirmed by the qRT-PCR analysis.

### Constructs generation and transformation

For the construction of *Pmex-5::ced-1*, *ced-1/Y47H9C.4a.1* was inserted in pPD95\_77 with *Pmex-5* (expressed in the germline) promoter. The transgene was performed by the cojunction of constructs (50  $\mu\text{g mL}^{-1}$ ) and marker construct (*Pdop-1::rfp*, 50  $\mu\text{g mL}^{-1}$ ) in the gonad.<sup>38</sup> Related primers are given in Table S3.†

### Data analysis

Using the SPSS Statistics 19.0 software, we performed the data analysis, and the data were presented as the mean  $\pm$  standard derivation (SD). The statistical significance of differences between treatments was examined using the one-way analysis of variance (ANOVA), followed by the post hoc test. Besides one-way ANOVA, two-way ANOVA was also carried out for comparing multiple factors.

## 3. Results and discussion

### Identification of germline GPCRs in response to NPS exposure

Previous studies have suggested that some genes encoding germline GPCRs (PAQR-2, GLC-1, SER-7, GLP-1 and CED-1) were potentially required for stress response.<sup>39–43</sup> After the exposure,

NPS (1–1000  $\mu\text{g L}^{-1}$ ) did not influence *glc-1*, *ser-7*, and *glp-1* expressions in the germline (Fig. 1B). However, exposure to NPS (1–1000  $\mu\text{g L}^{-1}$ ) increased the expressions of *paqr-2* and *ced-1* in the germline (Fig. 1B). In NPS (1–1000  $\mu\text{g L}^{-1}$ ) exposed *C. elegans*, an increase in the expression levels of *paqr-2* and *ced-1* in the germline was concentration-dependent (Fig. 1B).

### Germline RNAi knockdown of *ced-1* led to susceptibility to NPS toxicity

Using the DCL569 strain, the germline RNAi knockdown of *paqr-2* or *ced-1* could not result in a clear production of ROS, affected locomotion behavior, and influenced brood size under normal conditions (Fig. 2 and S1†). The germline RNAi knockdown of *paqr-2* did not influence the NPS toxicity (Fig. 2 and S1†). Different from this, the toxicity of NPS exposure in inducing ROS production, inhibiting locomotion behavior, and reducing brood size was enhanced by the germline RNAi knockdown of *ced-1* (Fig. 2 and S1†). Thus, the GPCR CED-1 function in the germline is to control the NPS toxicity. The efficiency for the germline RNAi knockdown of *paqr-2* or *ced-1* is shown in Fig. S2.†

### Target identification for germline CED-1 in controlling NPS toxicity

Potentially targeted genes of CED-1 have been raised during the control of different processes, and some of them can be expressed in the germline.<sup>44–49</sup> Among 16 potential targeted genes for germline *ced-1*, the germline RNAi knockdown of *ced-1* decreased the expression of CED-6, CED-10, DYN-1, VPS-34, LST-4, SNX-1, SNX-6, RAB-7, RAB-14, and EPN-1 in NPS-exposed DCL569 nematodes (Fig. 3A). Among these 10 candidate genes,

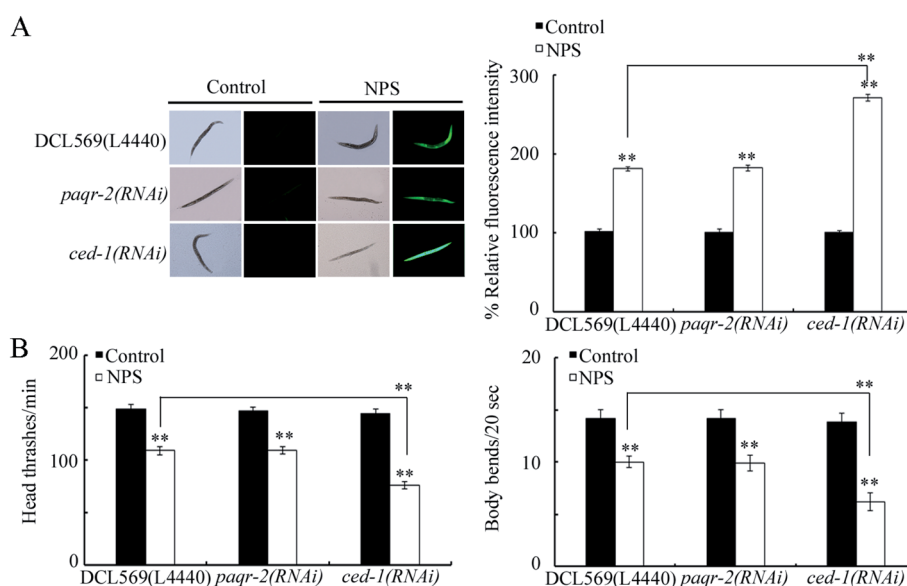
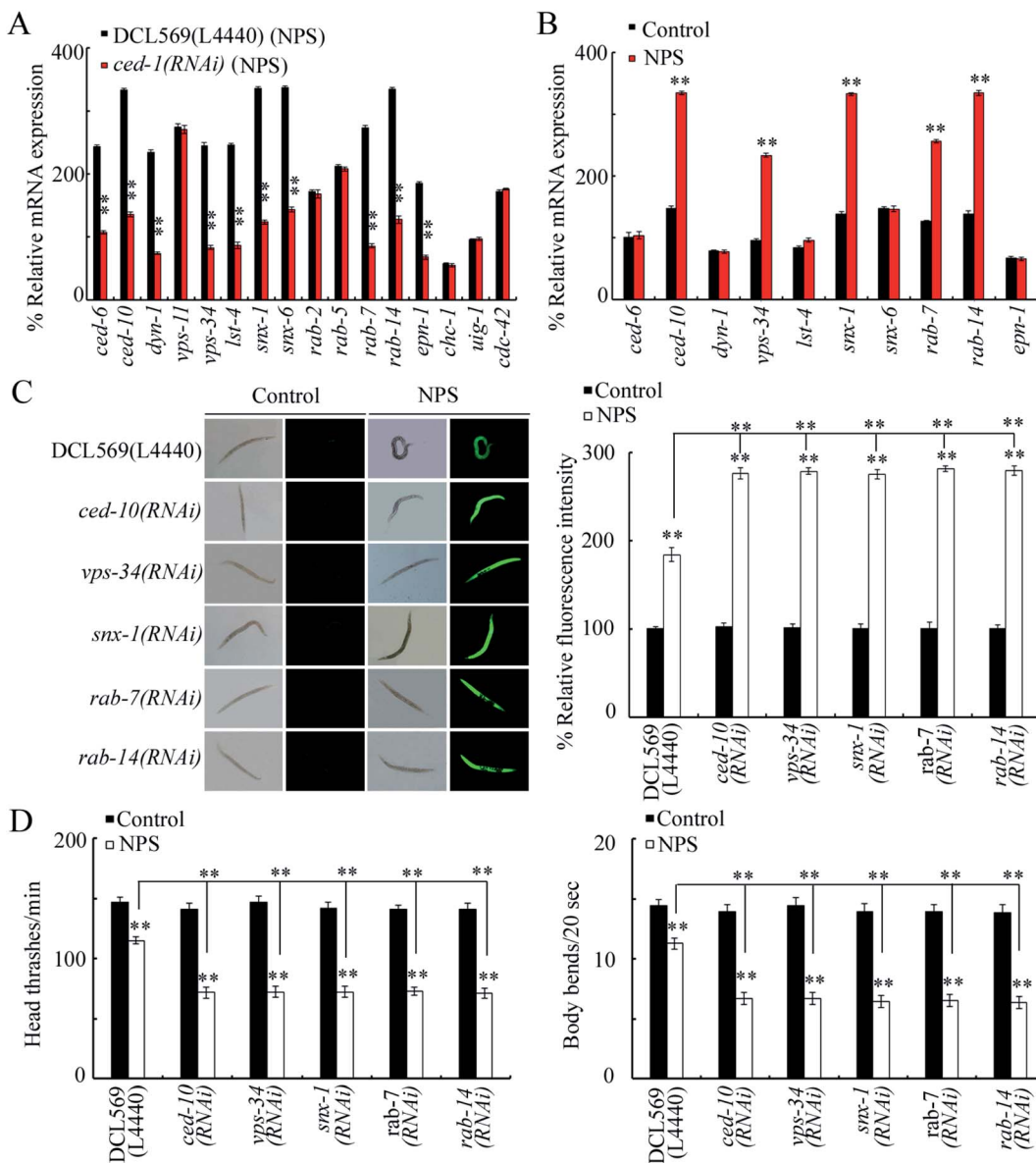


Fig. 2 Effect of the germline RNAi knockdown of *paqr-2* or *ced-1* on the toxicity of NPS. (A) Effect of the germline RNAi knockdown of *paqr-2* or *ced-1* on the toxicity of NPS in inducing ROS production. (B) Effect of the germline RNAi knockdown of *paqr-2* or *ced-1* on the toxicity of NPS in decreasing the locomotion behavior. The NPS exposure concentration was 1  $\mu\text{g L}^{-1}$ . Bars represent means  $\pm$  SD. \*\* $P < 0.01$  vs. control (if not specially indicated). If not specially indicated, the statistical significance of differences between treatments was examined using one-way ANOVA.





**Fig. 3** Identification of downstream targets of intestinal CED-1 in regulating the response to NPS exposure. (A) Effect of the germline RNAi knockdown of *ced-1* on gene expressions in NPS-exposed nematodes. L4440, empty vector. Bars represent means  $\pm$  SD. \*\* $P$  < 0.01 vs. DCL569. Statistical significance of differences between treatments was examined using one-way ANOVA. (B) Effect of NPS exposure on the expressions of CED-6, CED-10, DYN-1, VPS-34, LST-4, SNX-1, SNX-6, RAB-7, RAB-14, and EPN-1 in wild-type nematodes. Bars represent means  $\pm$  SD. \*\* $P$  < 0.01 vs. Control. Statistical significance of differences between treatments was examined using one-way ANOVA. (C) Effect of the germline RNAi knockdown of *ced-10*, *vps-34*, *snx-1*, *rab-7*, or *rab-14* on NPS toxicity in inducing ROS production. L4440, empty vector. Bars represent means  $\pm$  SD. \*\* $P$  < 0.01 vs. control (if not specially indicated). If not specially indicated, the statistical significance of differences between treatments was examined using one-way ANOVA. (D) Effect of the germline RNAi knockdown of *ced-10*, *vps-34*, *snx-1*, *rab-7*, or *rab-14* on NPS toxicity in decreasing locomotion behavior. L4440, empty vector. Bars represent means  $\pm$  SD. \*\* $P$  < 0.01 vs. control (if not specially indicated). If not specially indicated, the statistical significance of differences between treatments was examined using one-way ANOVA. The NPS exposure concentration was  $1 \mu\text{g L}^{-1}$ .

NPS ( $1 \mu\text{g L}^{-1}$ ) further increased the expression levels of CED-10, VPS-34, SNX-1, RAB-7, and RAB-14 in wild-type nematodes (Fig. 3B). In NPS exposed DCL569 worms, the germline RNAi knockdown of *ced-10*, *vps-34*, *snx-1*, *rab-7*, or *rab-14* caused severe production of ROS, suppression in the locomotion behavior, and reduction in the brood size (Fig. 3C, D and S3†), indicating the susceptibility of *ced-10(RNAi)*, *vps-34(RNAi)*, *snx-1(RNAi)*, *rab-7(RNAi)*, and *rab-14(RNAi)* animals towards NPS

toxicity. These findings implied the potential function of CED-10, VPS-34, SNX-1, RAB-7, and RAB-14 as targets for the germline CED-1 in controlling responses towards NPS exposure. *ced-10* encodes a small GTPase, *vps-34* encodes a VPS protein, *snx-1* encodes a BAR domain-containing sorting nexin, *rab-7* encodes a GTPase, and *rab-14* also encodes a GTPase. The efficiency for the germline RNAi knockdown of *ced-10*, *vps-34*, *snx-1*, *rab-7* or *rab-14* is shown in Fig. S4.†

## Genetic interaction between CED-1 and CED-10, VPS-34, SNX-1, RAB-7, or RAB-14 in the germline to control response to NPS exposure

To confirm the role of CED-10, VPS-34, SNX-1, RAB-7 or RAB-14 as the targets of the germline CED-1 in controlling NPS toxicity, we examined the genetic interaction between CED-1 and CED-10, VPS-34, SNX-1, RAB-7, or RAB-14 in the germline. The germline overexpression of CED-1 significantly suppressed the production of ROS, enhanced the locomotion behavior, and increased the brood size in NPS exposed worms (Fig. 4 and S5†), indicating the resistance of animals overexpressing germline CED-1 (*Is(Pmex-5-ced-1)*) to the NPS toxicity. Moreover, the RNAi knockdown of *ced-10*, *vps-34*, *snx-1*, *rab-7*, or *rab-14* could cause

a clear production of ROS, inhibition of the locomotion behavior, and reduction in the brood size in NPS exposed *Is(Pmex-5-ced-1)* worms (Fig. 4 and S5†), demonstrating that CED-10, VPS-34, SNX-1, RAB-7, and RAB-14 acted downstream of germline CED-1 to control the NPS toxicity.

## Effect of the germline RNAi knockdown of *ced-10*, *vps-34*, *snx-1*, *rab-7*, or *rab-14* on the expressions of genes encoding intestinal signaling

In *C. elegans*, the insulin, Wnt, p38 MAPK, and ELT-2 signaling pathways functioned in intestinal cells to control NPS toxicity.<sup>26,30,50,51</sup> In the insulin signaling pathway, DAF-16 is a FOXO transcriptional factor; in the Wnt signaling pathway,

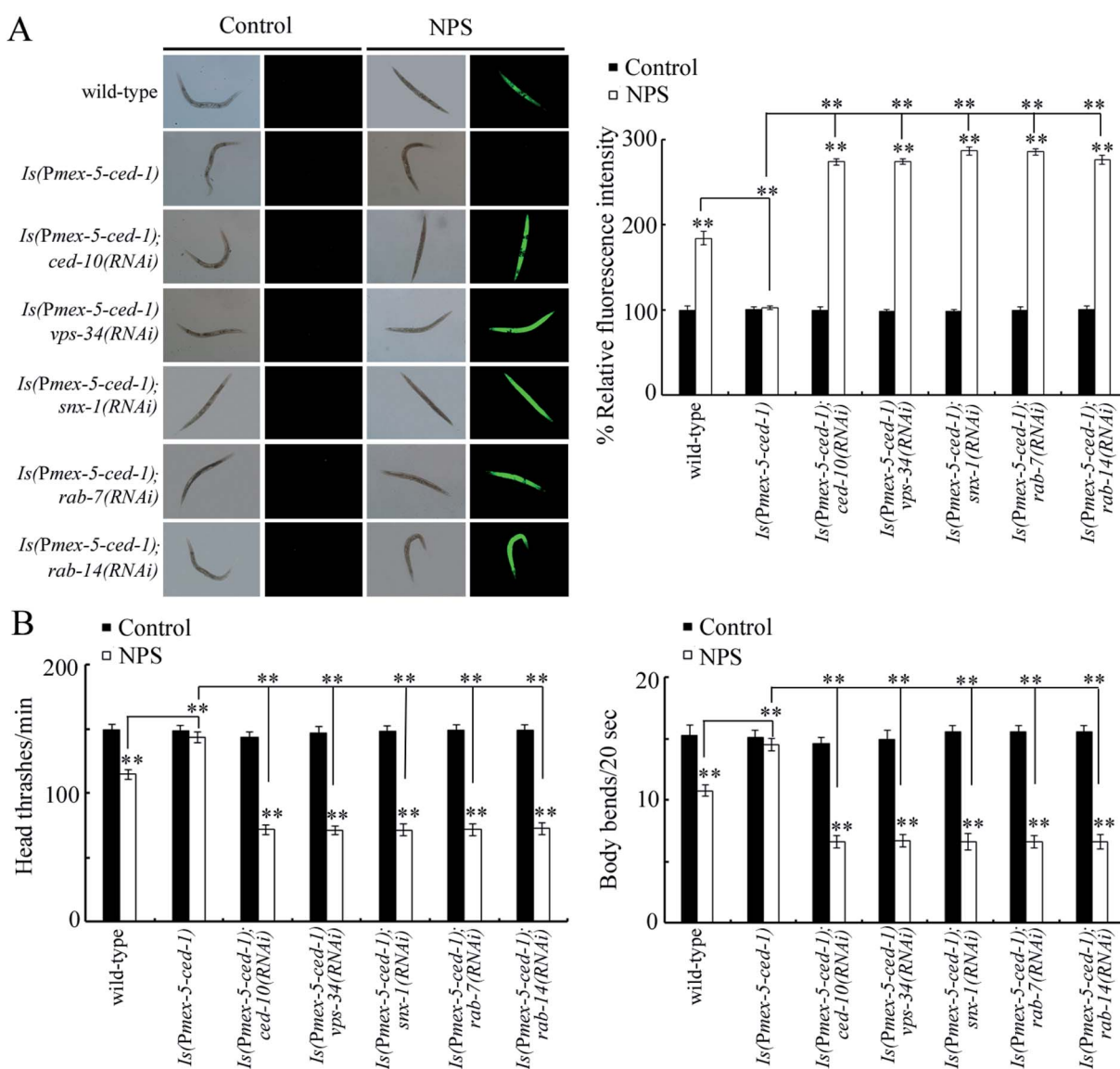


**Fig. 4** Genetic interactions between CED-1 and CED-10, VPS-34, SNX-1, RAB-7, or RAB-14 in the germline to regulate the response to NPS exposure. (A) Genetic interaction between CED-1 and CED-10, VPS-34, SNX-1, RAB-7, or RAB-14 in the germline to regulate the NPS toxicity in inducing ROS production. (B) Genetic interactions between CED-1 and CED-10, VPS-34, SNX-1, RAB-7, or RAB-14 in the germline to regulate the NPS toxicity in decreasing locomotion behavior. The exposure concentration of NPS was  $1 \mu\text{g L}^{-1}$ . Bars represent means  $\pm$  SD. \*\*P < 0.01 vs. control (if not specially indicated). If not specially indicated, the statistical significance of differences between treatments was examined using one-way ANOVA.

BAR-1 is a  $\beta$ -catenin transcriptional factor; and in the p38 MAPK signaling pathway, PMK-1 is a p38 MAPK. In insulin, Wnt, and p38 MAPK signaling pathways, only PMK-1/p38 MAPK and signaling cascades of DAF-2-AGE-1-AKT-1-DAF-16 and GSK-3-BAR-1 were found to be in response to NPS ( $1 \mu\text{g L}^{-1}$ ) exposure.<sup>26,30,50</sup> After NPS exposure, the germline RNAi knockdown of *ced-10*, *vps-34*, *snx-1*, *rab-7* or *rab-14* could not influence the expression levels of BAR-1 and *ELT-2* (Fig. 5A). In contrast, the germline RNAi knockdown of *ced-10*, *rab-7* or *rab-14* decreased the DAF-16 expression, and the germline RNAi knockdown of *vps-34* or *snx-1* decreased PMK-1 expression (Fig. 5A). Moreover,

we found that the germline RNAi knockdown of *ced-1* could further decrease the expression of DAF-16 and PMK-1 in NPS-exposed DCL569 worms (Fig. S6†). Nevertheless, after the NPS exposure, the germline RNAi knockdown of *ced-1* could not affect the expressions of BAR-1 and *ELT-2* (Fig. S6†).

During the regulation of stress response, the germline is an important organ.<sup>25</sup> In *C. elegans*, the bioavailable NPS particles were not only accumulated in the intestinal lumen but were also translocated and deposited in some reproductive organs, such as the gonad.<sup>20,21</sup> This observation implied that the NPS particles can directly activate the response of *C. elegans* in the

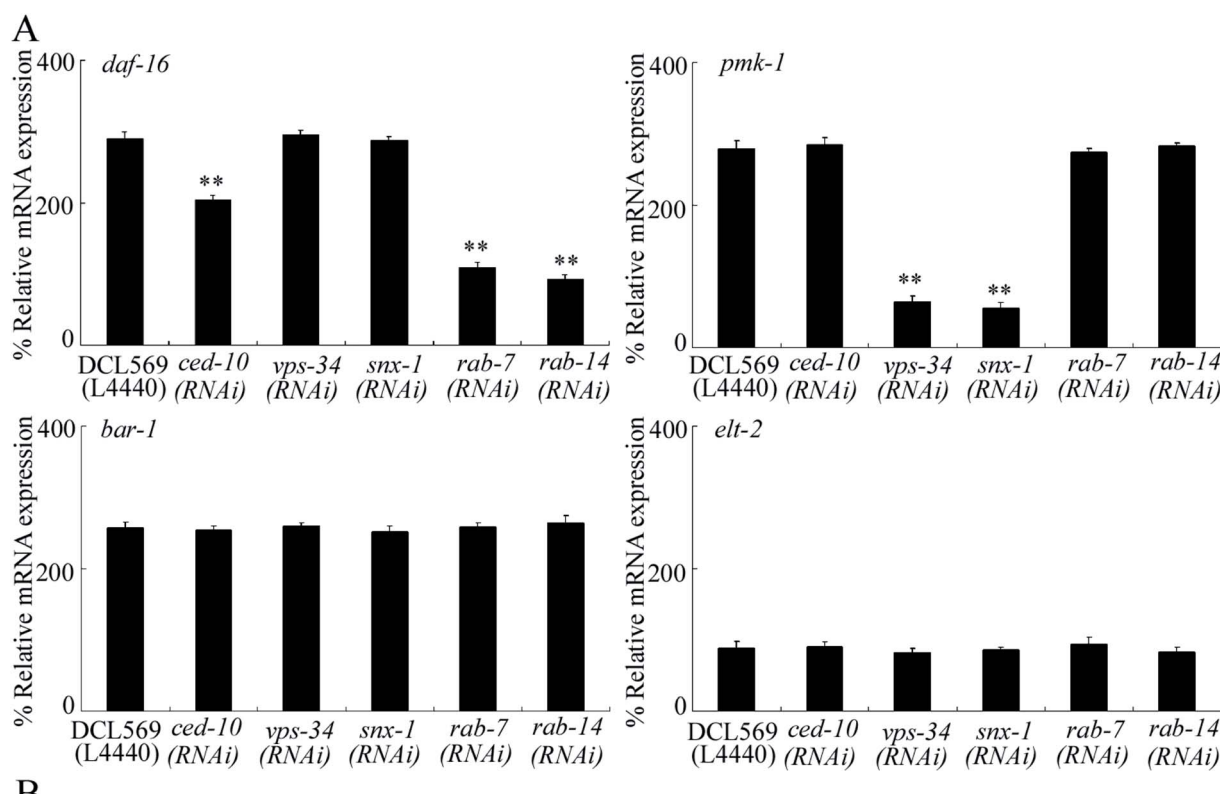


**Fig. 5** The germline RNAi knockdown of *ced-10*, *vps-34*, *snx-1*, *rab-7*, or *rab-14* affected expressions of DAF-16 and PMK-1 in NPS exposed DCL569 nematodes. (A) Effect of germline RNAi knockdown of *ced-10*, *vps-34*, *snx-1*, *rab-7*, or *rab-14* on expressions of *DAF-16*, *PMK-1*, *BAR-1*, and *ELT-2* in NPS exposed DCL569 nematodes. L4440, empty vector. The NPS exposure concentration was  $1 \mu\text{g L}^{-1}$ . Bars represent means  $\pm$  SD. \*\* $P < 0.01$  vs. DCL569. Statistical significance of differences between treatments was examined using one-way ANOVA. (B) A diagram showing the molecular basis for the germline CED-1 in response to NPS exposure in nematodes.

germline to NPS exposure. Nevertheless, there is still no direct evidence to support this assumption. Here, we found that NPS ( $1\text{--}1000\text{ }\mu\text{g L}^{-1}$ ) increased the expressions of two GPCRs in the germline (PAQR-2 and CED-1) (Fig. 1B). That is, a certain number of GPCRs can be activated in the germline by NPS exposure. This provides evidence for the existence of direct molecular response in the germline to NPS exposure in *C. elegans*.

For the two candidate germline GPCRs, the phenotype analysis indicated that only RNAi knockdown of *ced-1* affected the toxicity of NPS (Fig. 2 and S1†). The susceptibility could be observed in *ced-1(RNAi)* worms (Fig. 2 and S1†). Initially, CED-1 was identified to mediate the degradation and engulfment of cell corpses,<sup>52,53</sup> which indicates that CED-1 has the ability to recognize apoptotic cells by acting as a phagocyte receptor.<sup>54</sup> Due to this biological role, CED-1 is also required for the removal of neuronal debris during neuronal regeneration.<sup>55</sup> Moreover, CED-1 is involved in innate immunity control by activating the expression of genes for unfolded protein response.<sup>39</sup> In this study, our results further demonstrated that GPCR CED-1 in the germline can control the stress response by mediating a protective response towards certain toxicants such as NPS (Fig. 5B).

During the control of NPS toxicity, we provided several lines of evidence to prove the roles of CED-10, VPS-34, SNX-1, RAB-7, and RAB-14 as downstream targets activated by GPCR CED-1 in the germline in controlling NPS toxicity. First, the genes encoding these five proteins could be increased by NPS exposure (Fig. 3B) and decreased in NPS exposed *ced-1(RNAi)* worms (Fig. 3A). Second, the susceptibility to NPS toxicity could be detected in *ced-10(RNAi)*, *vps-34(RNAi)*, *snx-1(RNAi)*, *rab-7(RNAi)*, and *rab-14(RNAi)* worms (Fig. 3C, D and S3†). More importantly, the resistance of *Is(Pmex-5-ced-1)* worms towards NPS toxicity was inhibited by the RNAi knockdown of *ced-10*, *vps-34*, *snx-1*, *rab-7*, and *rab-14* (Fig. 4 and S5†). During the removal of cell corpses, CED-10 linked different engulfment pathways by functioning downstream of CED-7, CED-6 and CED-1.<sup>56</sup> During the phagolysosome formation, RAB-7 was a downstream effector of CED-1.<sup>57</sup> VPS-34 and RAB-14 functioned in an ordered manner downstream of CED-1 to control phagosome maturation.<sup>46,49,58</sup> SNX-1 (a nexin) was required in driving the degradation of cell corpses in the signaling cascade initiated by CED-1.<sup>48</sup> Here, we further raised the signaling cascade of CED-1–CED-10/VPS-34/SNX-1/RAB-7/RAB-14 in the germline to control NPS toxicity, which strengthened the understanding of the molecular basis for the germline in response to exposure to toxicants such as NPS (Fig. 5B). Nevertheless, the molecular basis for the germline in response to NPS exposure was still very limited. Future work on the elucidation of molecular signals mediated by germline CED-10, VPS-34, SNX-1, RAB-7 and RAB-14 in controlling NPS toxicity is needed.

In *C. elegans*, during the degradation and engulfment of the apoptotic cell, CED-6 (an adaptor protein) and DYN-1 (a GTPase dynamin) mediate the CED-1 function.<sup>52,59</sup> At the early step, LST-4 promoted the phagosome maturation process.<sup>46</sup> SNX-6 is another nexin in the signaling cascade initiated by CED-1 to regulate the degradation of cell corpses.<sup>48</sup> EPN-1 (an adaptor

epsin) functioned in the same CED-1 pathway to control cell corpse engulfment.<sup>45</sup> We further observed that besides the expression levels of CED-10, VPS-34, SNX-1, RAB-7, and RAB-14, the expression levels of CED-6, DYN-1, LST-4, SNX-6, and EPN-1 were also inhibited in 100 nm NPS exposed *ced-1(RNAi)* worms (Fig. 3A). In *C. elegans*, the smaller NPS particles induced more severe toxic effects than polystyrene having large sizes.<sup>60</sup> Doses ( $\leq 1\text{ }\mu\text{g L}^{-1}$ ) have been raised as predicted environmental doses for NP particles.<sup>61</sup> Thus, CED-6, DYN-1, LST-4, SNX-6 and EPN-1 may also potentially function downstream of the germline GPCR CED-1 to control the toxicity of NPS with the smaller size and at the predicted environmental concentration.

Furthermore, we found the germline-intestine communication mediated by CED-6, DYN-1, LST-4, SNX-6, and EPN-1 during the control of NPS toxicity (Fig. 5B). In NPS-exposed nematodes, the expressions of DAF-16 and PMK-1 could be inhibited in *ced-10(RNAi)*, *vps-34(RNAi)*, *snx-1(RNAi)*, *rab-7(RNAi)* or *rab-14(RNAi)* worms (Fig. 5A). Previous studies have indicated that the functions of both p38 MAPK and insulin signaling pathways in controlling NPS toxicity were only restricted in the intestinal cells.<sup>28,30</sup> Therefore, CED-1 activated signaling cascade in the germline could control the NPS toxicity by affecting the activities of p38 MAPK and insulin signaling pathways in the intestinal cells. That is, besides the neuron-intestine communication,<sup>52,63</sup> the germline-intestine communication is further required for controlling NPS toxicity.

## 4. Conclusions

Together, we examined the GPCRs in the germline in response to NPS exposure. We detected two GPCRs in the germline (PAQR-2 and CED-1) activated by NPS ( $1\text{--}1000\text{ }\mu\text{g L}^{-1}$ ). After the NPS exposure, the increase in the germline GPCR CED-1 mediated a protective response. CED-1 mediated this protective response to NPS exposure by activating the downstream five targets (CED-10, VPS-34, SNX-1, RAB-7, and RAB-14). Moreover, these five germline targets further controlled the NPS toxicity by affecting the functions of p38 MAPK and insulin signaling pathways in the intestine. Our findings strengthened the understanding of the molecular basis for the germline in response to NPS exposure.

## Conflicts of interest

There are no conflicts to declare.

## References

- 1 D. K. A. Barnes, F. Galgani, R. C. Thompson and M. Barlaz, Accumulation and fragmentation of plastic debris in global environments, *Philos. Trans. R. Soc., B*, 2009, **364**, 1985–1998.
- 2 S. Lambert and M. Wagner, Characterisation of nanoplastics during the degradation of polystyrene, *Chemosphere*, 2016, **145**, 265–268.
- 3 Y. Chae and Y. J. An, Effects of micro- and nanoplastics on aquatic ecosystems: current research trends and perspectives, *Mar. Pollut. Bull.*, 2017, **124**, 624–632.



4 J. Saavedra, S. Stoll and V. I. Slaveykova, Influence of nanoplastic surface charge on eco-corona formation, aggregation and toxicity to freshwater zooplankton, *Environ. Pollut.*, 2019, **252**, 715–722.

5 S. B. Sjollema, P. Redondo-Hasselerharm, H. A. Leslie, M. H. S. Kraak and A. D. Vethaak, Do plastic particles affect microalgal photosynthesis and growth?, *Aquat. Toxicol.*, 2016, **170**, 259–261.

6 L. Canesi, C. Ciacci, E. Bergami, M. P. Monopoli, K. A. Dawson, S. Papa, B. Canonico and I. Corsi, Evidence for immunomodulation and apoptotic processes induced by cationic polystyrene nanoparticles in the hemocytes of the marine bivalve *Mytilus*, *Mar. Environ. Res.*, 2015, **111**, 34–40.

7 L. G. A. Barboza, L. R. Vieira and L. Guilhermino, Single and combined effects of microplastics and mercury on juveniles of the European seabass (*Dicentrarchus labrax*): changes in behavioural responses and reduction of swimming velocity and resistance time, *Environ. Pollut.*, 2018, **236**, 1014–1019.

8 Y. Jin, J. Xia, Z. Pan, J. Yang, W. Wang and Z. Fu, Polystyrene microplastics induce microbiota dysbiosis and inflammation in the gut of adult zebrafish, *Environ. Pollut.*, 2018, **235**, 322–329.

9 T. Kögel, Ø. Bjørøy, B. Toto, A. M. Bienfait and M. Sanden, Micro- and nanoplastic toxicity on aquatic life: determining factors, *Sci. Total Environ.*, 2020, **709**, 136050.

10 Y. Yu, H. Chen, X. Hua, Y. Dang, Y. Han, Z. Yu, X. Chen, P. Ding and H. Li, Polystyrene microplastics (PS-MPs) toxicity induced oxidative stress and intestinal injury in nematode *Caenorhabditis elegans*, *Sci. Total Environ.*, 2020, **726**, 138679.

11 T. Zheng, D. Yuan and C. Liu, Molecular toxicity of nanoplastics involving in oxidative stress and deoxyribonucleic acid damage, *J. Mol. Recognit.*, 2019, **32**, e2804.

12 A. Cózar, F. Echevarría, J. Ignacio González-Gordillo, X. Irigoien, B. Úbeda, S. Hernández-León, A. T. Palma, S. Navarro, J. García-de-Lomas, A. Ruiz, M. L. Fernández-de-Puelles and C. M. Duarte, Plastic debris in the open ocean?, *Proc. Natl. Acad. Sci. U. S. A.*, 2014, **111**, 10239–10244.

13 R. Lehner, C. Weder, A. Petri-Fink and B. Rothen-Rutishauser, Emergence of nanoplastic in the environment and possible impact on human health, *Environ. Sci. Technol.*, 2019, **53**, 1748–1765.

14 H. M. Kim, D. K. Lee, N. P. Long, S. W. Kwon and J. H. Park, Uptake of nanopolystyrene particles induces distinct metabolic profiles and toxic effects in *Caenorhabditis elegans*, *Environ. Pollut.*, 2019, **246**, 578–586.

15 S. W. Kim, D. Kim, S. Jeong and Y. An, Size-dependent effects of polystyrene plastic particles on the nematode *Caenorhabditis elegans* as related to soil physicochemical properties, *Environ. Pollut.*, 2020, **258**, 113740.

16 D.-Y. Wang, *Exposure Toxicology in Caenorhabditis elegans*, Springer Nature Singapore Pte Ltd, 2020.

17 M. Qu, Y.-X. Qiu, Y. Kong and D.-Y. Wang, Amino modification enhances reproductive toxicity of nanopolystyrene on gonad development and reproductive capacity in nematode *Caenorhabditis elegans*, *Environ. Pollut.*, 2019, **254**, 112978.

18 M. Qu and D.-Y. Wang, Toxicity comparison between pristine and sulfonate modified nanopolystyrene particles in affecting locomotion behavior, sensory perception, and neuronal development in *Caenorhabditis elegans*, *Sci. Total Environ.*, 2020, **703**, 134817.

19 L. Lei, S. Wu, S. Lu, M. Liu, Y. Song, Z. Fu, H. Shi, K. H. Raley-Susman and D. He, Microplastic particles cause intestinal damage and other adverse effects in zebrafish *Danio rerio* and nematode *Caenorhabditis elegans*, *Sci. Total Environ.*, 2018, **619–620**, 1–8.

20 L. Zhao, M. Qu, G. Wong and D.-Y. Wang, Transgenerational toxicity of nanopolystyrene particles in the range of  $\mu\text{g/L}$  in nematode *Caenorhabditis elegans*, *Environ. Sci.: Nano*, 2017, **4**, 2356–2366.

21 M. Qu, K.-N. Xu, Y.-H. Li, G. Wong and D.-Y. Wang, Using *acs-22* mutant *Caenorhabditis elegans* to detect the toxicity of nanopolystyrene particles, *Sci. Total Environ.*, 2018, **643**, 119–126.

22 K. Gamo, S. Kiryu-Seo, H. Konishi, S. Aoki, K. Matsushima, K. Wada and H. Kiyama, G-protein-coupled receptor screen reveals a role for chemokine receptor CCR5 in suppressing microglial neurotoxicity, *J. Neurosci.*, 2008, **28**, 11980–11988.

23 C. Jee, J. Lee, J. P. Lim, D. Parry, R. O. Messing and S. L. McIntire, SEB-3, a CRF receptor-like GPCR, regulates locomotor activity states, stress responses and ethanol tolerance in *Caenorhabditis elegans*, *Genes, Brain Behav.*, 2013, **12**, 250–262.

24 D.-Y. Wang, *Molecular Toxicology in Caenorhabditis elegans*, Springer Nature Singapore Pte Ltd, 2019.

25 D.-Y. Wang, *Target Organ Toxicology in Caenorhabditis elegans*, Springer Nature Singapore Pte Ltd, 2019.

26 H.-M. Shao, Z.-Y. Han, N. Krasteva and D.-Y. Wang, Identification of signaling cascade in the insulin signaling pathway in response to nanopolystyrene particles, *Nanotoxicology*, 2019, **13**, 174–188.

27 P. Sen, Y. Xiong, Q. Zhang, S. Park, W. You, H. Ade, M. W. Kudenov and B. T. O'Connor, Shear-enhanced transfer printing of conducting polymer thin films, *ACS Appl. Mater. Interfaces*, 2018, **10**, 31560.

28 H. Gelbke, M. Banton, C. Block, G. Dawkins, R. Eisert, E. Leibold, M. Pemberton, I. M. Puijk, A. Sakoda and A. Yasukawa, Risk assessment for migration of styrene oligomers into food from polystyrene food containers, *Food Chem. Toxicol.*, 2019, **124**, 151–167.

29 M. A. Abdallah, M. Sharkey, H. Berresheim and S. Harrad, Hexabromocyclododecane in polystyrene packaging: a downside of recycling?, *Chemosphere*, 2018, **199**, 612–616.

30 M. Qu, Y.-Q. Liu, K.-N. Xu and D.-Y. Wang, Activation of p38 MAPK signaling-mediated endoplasmic reticulum unfolded protein response by nanopolystyrene particles, *Adv. Biosyst.*, 2019, **3**, 1800325.

31 Y.-H. Yang, H.-H. Du, G.-S. Xiao, Q.-L. Wu and D.-Y. Wang, Response of intestinal  $\text{G}\alpha$  subunits to nanopolystyrene in nematode *Caenorhabditis elegans*, *Environ. Sci.: Nano*, 2020, **7**, 2351–2359.



32 S. Brenner, The genetics of *Caenorhabditis elegans*, *Genetics*, 1974, **77**, 71–94.

33 Y.-H. Yang, Q.-L. Wu and D.-Y. Wang, Epigenetic response to nanopolystyrene in germline of nematode *Caenorhabditis elegans*, *Ecotoxicol. Environ. Saf.*, 2020, **206**, 111404.

34 Y.-X. Qiu, Y.-Q. Liu, Y.-H. Li and D.-Y. Wang, Intestinal *mir-794* responds to nanopolystyrene by linking insulin and p38 MAPK signaling pathways in nematode *Caenorhabditis elegans*, *Ecotoxicol. Environ. Saf.*, 2020, **201**, 110857.

35 H.-L. Liu, D. Li, R.-J. Zhang, L.-M. Sun and D.-Y. Wang, Lipid metabolic sensors of MDT-15 and SBP-1 regulated the response to simulated microgravity in the intestine of *Caenorhabditis elegans*, *Biochem. Biophys. Res. Commun.*, 2020, **528**, 28–34.

36 L.-M. Sun, W.-J. Li, D. Li and D.-Y. Wang, microRNAs involved in the control of toxicity on locomotion behavior induced by simulated microgravity stress in *Caenorhabditis elegans*, *Sci. Rep.*, 2020, **10**, 17510.

37 L. Zou, D. Wu, X. Zang, Z. Wang, Z. Wu and D. Chen, Construction of a germline-specific RNAi tool in *C. elegans*, *Sci. Rep.*, 2019, **9**, 2354.

38 D. Li, Y.-J. Yuan and D.-Y. Wang, Regulation of response to nanopolystyrene by intestinal microRNA *mir-35* in nematode *Caenorhabditis elegans*, *Sci. Total Environ.*, 2020, **736**, 139677.

39 K. A. Haskins, J. F. Russell, N. Gaddis, H. K. Dressman and A. Aballay, Unfolded protein response genes regulated by CED-1 are required for *Caenorhabditis elegans* innate immunity, *Dev. Cell*, 2008, **15**, 87–97.

40 K. Singh, M. Y. Chao, G. A. Somers, H. Komatsu, M. E. Corkins, J. Larkins-Ford, T. Tucey, H. M. Dionne, M. B. Walsh, E. K. Beaumont, D. P. Hart, S. Lockery and A. C. Hart, *C. elegans* notch signaling regulates adult chemosensory response and larval molting quiescence, *Curr. Biol.*, 2011, **21**, 825–834.

41 R. Ghosh, E. C. Andersen, J. A. Shapiro, J. P. Gerke and L. Kruglyak, Natural variation in a chloride channel subunit confers avermectin resistance in *C. elegans*, *Science*, 2012, **335**, 574–578.

42 E. Svensk, R. Devkota, M. Ståhlman, P. Ranji, M. Rauthan, F. Magnusson, S. Hammarsten, M. Johansson, J. Boren and M. Pilon, *Caenorhabditis elegans* PAQR-2 and IGLR-2 protect against glucose toxicity by modulating membrane lipid composition, *PLoS Genet.*, 2016, **12**, e1005982.

43 R. Pocock and O. Hobert, Hypoxia activates a latent circuit for processing gustatory information in *C. elegans*, *Nat. Neurosci.*, 2010, **13**, 610–614.

44 L. J. Neukomm, S. Zeng, A. P. Frei, P. A. Huegli and M. O. Hengartner, Small GTPase CDC-42 promotes apoptotic cell corpse clearance in response to PAT-2 and CED-1 in *C. elegans*, *Cell Death Differ.*, 2014, **21**, 845–853.

45 Q. Shen, B. He, N. Lu, B. Conradt, B. D. Grant and Z. Zhou, Phagocytic receptor signaling regulates clathrin and epsin mediated cytoskeletal remodeling during apoptotic cell engulfment in *C. elegans*, *Development*, 2013, **140**, 3230–3243.

46 D. Chen, Y. Jian, Z. Liu, Y. Zhang, J. Liang, X. Qi, H. Du, W. Zou, L. Chen, Y. Chai, G. Ou, L. Miao, Y. Wang and C. Yang, Clathrin and AP2 are required for phagocytic receptor-mediated apoptotic cell clearance in *Caenorhabditis elegans*, *PLoS Genet.*, 2013, **9**, e1003517.

47 L. J. Neukomm, A. Nicot, J. M. Kinchen, J. Almendinger, S. M. Pinto, S. Zeng, K. Doukoumetzidis, H. Tronchère, B. Payrastre, J. F. Laporte and M. O. Hengartner, The phosphoinositide phosphatase MTM-1 regulates apoptotic cell corpse clearance through CED-5-CED-12 in *C. elegans*, *Development*, 2011, **138**, 2003–2014.

48 N. Lu, Q. Shen, T. R. Mahoney, X. Liu and Z. Zhou, Three sorting nexins drive the degradation of apoptotic cells in response to PtdIns(3)P signaling, *Mol. Biol. Cell*, 2011, **22**, 354–374.

49 J. M. Kinchen, K. Doukoumetzidis, J. Almendinger, L. Stergiou, A. Tosello-Trampont, C. D. Sifri, M. O. Hengartner and K. S. Ravichandran, A novel pathway for phagosome maturation during engulfment of apoptotic cells, *Nat. Cell Biol.*, 2008, **10**, 556–566.

50 H.-M. Shao, Y. Kong and D.-Y. Wang, Response of intestinal signaling communication between nucleus and peroxisome to nanopolystyrene at predicted environmental concentration, *Environ. Sci.: Nano*, 2020, **7**, 250–261.

51 H.-M. Shao and D.-Y. Wang, Long-term and low-dose exposure to nanopolystyrene induces a protective strategy to maintain functional state of intestine barrier in nematode *Caenorhabditis elegans*, *Environ. Pollut.*, 2020, **258**, 113649.

52 X. Yu, S. Odera, C. H. Chuang, N. Lu and Z. Zhou, *C. elegans* dynamin mediates the signaling of phagocytic receptor CED-1 for the engulfment and degradation of apoptotic cells, *Dev. Cell*, 2006, **10**, 743–757.

53 Z. Zhou, E. Hartwig and H. R. Horvitz, CED-1 is a transmembrane receptor that mediates cell corpse engulfment in *C. elegans*, *Cell*, 2001, **104**, 43–56.

54 X. Wang, W. Li, D. Zhao, B. Liu, Y. Shi, B. Chen, H. Yang, P. Guo, X. Geng, Z. Shang, E. Peden, E. Kage-Nakadai, S. Mitani and D. Xue, *Caenorhabditis elegans* transthyretin-like protein TTR-52 mediates recognition of apoptotic cells by the CED-1 phagocyte receptor, *Nat. Cell Biol.*, 2010, **12**, 655–664.

55 H. Chiu, Y. Zou, N. Suzuki, Y. Hsieh, C. Chuang, Y. Wu and C. Chang, Engulfing cells promote neuronal regeneration and remove neuronal debris through distinct biochemical functions of CED-1, *Nat. Commun.*, 2018, **9**, 4842.

56 J. M. Kinchen, J. Cabello, D. Klingele, K. Wong, R. Feichtinger, H. Schnabel, R. Schnabel and M. O. Hengartner, Two pathways converge at CED-10 to mediate actin rearrangement and corpse removal in *C. elegans*, *Nature*, 2005, **434**, 93–99.

57 X. Yu, N. Lu and Z. Zhou, Phagocytic receptor CED-1 initiates a signaling pathway for degrading engulfed apoptotic cells, *PLoS Biol.*, 2008, **6**, e61.

58 P. Guo, T. Hu, J. Zhang, S. Jiang and X. Wang, Sequential action of *Caenorhabditis elegans* Rab GTPases regulates phagolysosome formation during apoptotic cell



degradation, *Proc. Natl. Acad. Sci. U. S. A.*, 2010, **107**, 18016–18021.

59 H. P. Su, K. Nakada-Tsukui, A. Tosell-Trampont, Y. Li, G. Bu, P. M. Henson and K. S. Ravichandran, Interaction of CED-6/GULP, an adapter protein involved in engulfment of apoptotic cells with CED-1 and CD91/low density lipoprotein receptor-related protein (LRP), *J. Biol. Chem.*, 2002, **277**, 11772–11779.

60 Y.-X. Qiu, Y.-Q. Liu, Y.-H. Li, G.-J. Li and D.-Y. Wang, Effect of chronic exposure to nanopolystyrene on nematode *Caenorhabditis elegans*, *Chemosphere*, 2020, **256**, 127172.

61 R. Lenz, K. Enders and T. G. Nielsen, Microplastic exposure studies should be environmentally realistic, *Proc. Natl. Acad. Sci. U. S. A.*, 2016, **113**, E4121–E4122.

62 H.-L. Liu, R.-J. Zhang and D.-Y. Wang, Response of DBL-1/TGF- $\beta$  signaling-mediated neuron-intestine communication to nanopolystyrene in nematode *Caenorhabditis elegans*, *Sci. Total Environ.*, 2020, **745**, 141047.

63 S.-T. Wang, H.-L. Liu, Y.-Y. Zhao, Q. Rui and D.-Y. Wang, Dysregulated *mir-354* enhanced the protective response to nanopolystyrene by affecting the activity of TGF- $\beta$  signaling pathway in nematode *Caenorhabditis elegans*, *NanoImpact*, 2020, **20**, 100256.

